

Study of superconducting properties of MgB_2

Y. Machida* and S. Sasaki

*Materials and Structures Laboratory, Tokyo Institute of Technology
4259 Nagatsuta, Midori-ku, Yokohama 226-8503, Japan*

H. Fujii

National Institute for Materials Science, 1-2-1, Sengen, Tsukuba 305-0047, Japan

M. Furuyama, I. Kakeya and K. Kadowaki

*Institute of Materials Science, University of Tsukuba, 1-1-1, Tennoudai, Tsukuba 305-8573, Japan
(Dated: December 30, 2021)*

We synthesized single crystalline and polycrystalline MgB_2 under ambient pressures. The single crystals of MgB_2 were of good quality, where the crystal structure refinements were successfully converged with $R=0.020$. The specific heat of polycrystalline MgB_2 samples has been measured in a temperature range between 2 and 60 K in magnetic field up to 6 T. The measurement gave the coefficient of the linear term in the electronic specific heat, $\gamma=3.51 \text{ mJ/K}^2 \text{ mol}$, and the jump of the specific heat, $2.8 \text{ mJ/K}^2 \text{ mol}$ at 38.5 K. It is shown from the analysis of the specific heat that the electronic specific heat in the superconducting state differs largely from the conventional BCS weak coupling theory. From the results of measurements of the magnetic properties on single crystal samples, we found a sharp superconducting transition at 38 K with transition width $\Delta T_c=0.8 \text{ K}$ and the superconducting anisotropy ratio γ increasing from about 1 near T_c to 4.0 at 25 K.

PACS numbers: 74.25.Bt, 74.25.Ha, 74.62.Bf, 74.60.Ec

The recent discovery of superconductivity at 39 K in magnesium diboride MgB_2 ¹ has attracted great scientific interest. Several experiments indicated a phonon-mediated *s*-wave BCS superconductivity^{2,3} and the appearance of a double energy gap was predicted^{4,5}. Specific heat⁶ and spectroscopic⁷ measurements, scanning tunneling spectroscopy^{8,9} gave evidence for this prediction. However, several key parameters such as the upper critical fields H_{c2} and their anisotropy ratio γ , the magnetic penetration λ , the coherence lengths ξ and Ginzburg-Landau parameters κ are not well established because of the difficulty of growing high quality MgB_2 single crystals. Especially the anisotropy ratio $\gamma=H_{c2}^{ab}/H_{c2}^c$ is important to clarify the superconducting mechanism and applications of MgB_2 . Here H_{c2}^{ab} and H_{c2}^c are the in-plane and the out-of-plane upper critical fields respectively. Reported γ -values vary widely depending on the measurement methods or on the sample types. The values determined from resistivity on polycrystalline¹⁰, aligned crystallites¹¹, *c*-axis oriented films^{12,13,14} and single crystals^{15,16,17,18,19,20,21,22} have been reported to be 6-9, 1.7, 1.3-2 and 2.6-3, respectively.

In this paper, we present a study of the specific and the magnetization measurements on single crystalline and polycrystalline MgB_2 . The polycrystals for the specific measurement were synthesized as follows. The Mg (99.99%, Furuya Metal Co.) ingot and the B (99.9%, Furuchi Chemical Co.) powder were pressed into a cylinder with a diameter of 13 mm and a length of 15 mm. This was put in the BN crucible with a lid, and this crucible was encapsulated in a stainless (SUS304) tube in argon atmosphere. Then, this was reacted for three

hours at 1100°C in an electric furnace. The sample after reaction was a form of sintered porous lump. This was not so hard that the sample was cut from this lump in a shape of thin, square plate for the specific heat measurement.

The single crystals were grown in the stainless (SUS304) tube. The SUS304 tube had an outside diameter of 32 mm, a wall thickness of 1.5 mm, and a length of 110 mm. The inner surface of the tube was sealed by Mo sheet (99.95%, Nilaco Co.) with the size of $0.05 \times 100 \times 200 \text{ mm}^3$. One end of the SUS304 tube was pressed with a vise and sealed in an Ar gas atmosphere by arc welding. The starting materials of Mg chunk with the size of 3~5 mm and B chunk which was cut out with the size of about 1 cm^3 from B block was filled inside of the tube. Then the other end of the tube was pressed with a vise and sealed in an Ar gas atmosphere by arc welding, as well. The samples were heated from room temperature to 1200°C for 40 minutes and kept at 1200°C for 12 hours, then slowly cooled to room temperature for 12 hours. The single crystals finally obtained were about $100 \sim 300 \mu\text{m}$, which had irregular shapes with shiny gold color when observed under a optical microscope.

The single crystal images observed by a scanning electron microscope (SEM) is shown in Fig 1(a). The crystals were found to have very flat surfaces. Structural analysis was carried out using a x-ray precession camera, a four-circle diffractometer and a transmission electron microscope (TEM). The x-ray precession photograph indicated that the crystal has the hexagonal structure, as shown in Fig 1(b). The diffraction data were collected by using graphite monochromated MoK_α radiation at room temperature and refined by

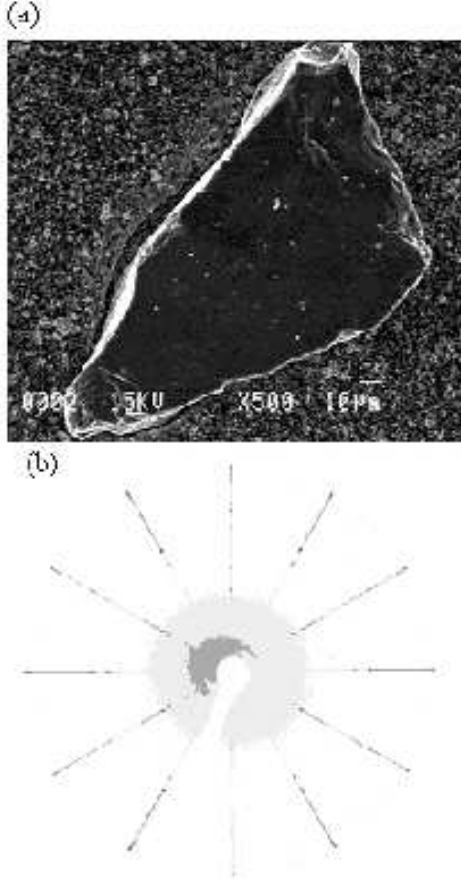


FIG. 1: (a) SEM image of a MgB_2 single crystal with a size of about $100\ \mu\text{m}$. (b) X-ray precession photograph of the single crystal.

the least-square procedure using 86 reflections as the average of the measured 866 reflections. The obtained cell and structural parameters were $a = b = 3.0863(4)\ \text{\AA}$, $c = 3.5178(4)\ \text{\AA}$, $(x,y,z) = (0,0,0)$ (Mg), $(1/3, 2/3, 1/2)$ (B), $U_{11}(\text{Mg}) = 0.0078(2)\ \text{\AA}^2$, $U_{33}(\text{Mg}) = 0.0054(2)\ \text{\AA}^2$, $B_{eq}(\text{Mg}) = 0.382(2)\ \text{\AA}^2$, $U_{11}(\text{B}) = 0.0068(2)\ \text{\AA}^2$, $U_{33}(\text{B}) = 0.0058(2)\ \text{\AA}^2$ and $B_{eq}(\text{B}) = 0.371(2)\ \text{\AA}^2$ with small agreement factors $R = 0.020$, $R_w = 0.027$ ($w = \text{weight}$). To confirm the structure of the MgB_2 phase, we took plane-view HRTEM images and electron diffraction patterns in selected areas for beam directions of $[001]$ and $[100]$ as shown in Fig 2, which indicated atomic arrangement with $P6/mmm$ cell of MgB_2 . Neither extra spots nor streaks were found, indicating that the crystal is of high quality.

The temperature dependence of the magnetization curve was measured at $1\ \text{mT}$ along the c -axis and the ab -plane by a superconducting quantum interference device (SQUID) magnetometer. Figure 3(a) is the results for the MgB_2 single crystal. It shows the $M(T)$ curves in the zero-field-cooling (ZFC) and the field-cooling (FC) modes. The onset of superconducting transition was ob-

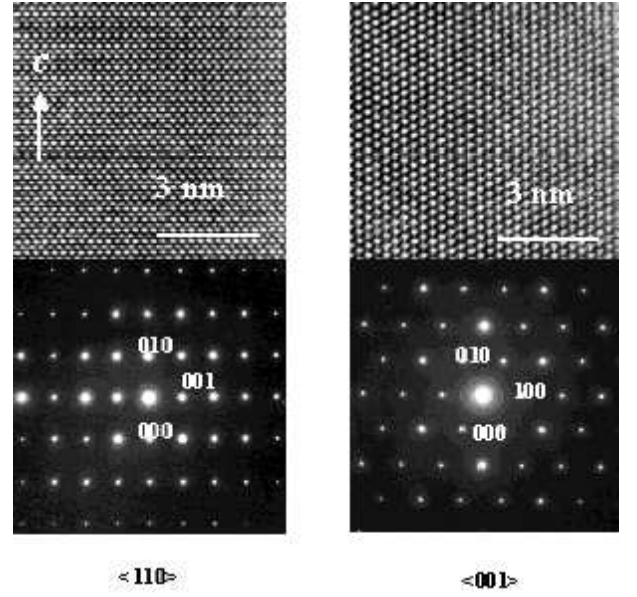


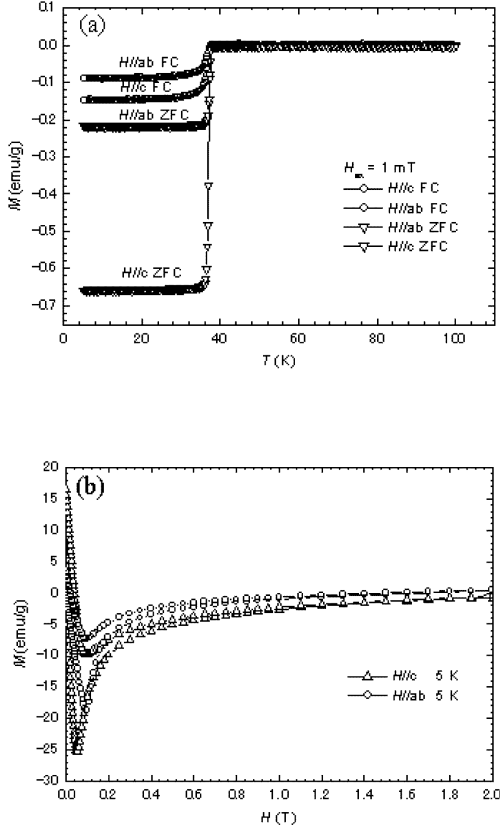
FIG. 2: Electron diffraction patterns and HRTEM images of a MgB_2 single crystal for a beam direction of $[001]$ and $[110]$ in the hexagonal structure.

served at $T_c = 38\ \text{K}$ with transition width $\Delta T_c = 0.8\ \text{K}$ both for $H//ab$ and for $H//c$, indicating high quality of the samples, where $//ab$ ($//c$) indicates the field H perpendicular (parallel) to the c -axis of the sample, respectively. Comparing to the transition temperatures ($\approx 39\ \text{K}$) for polycrystal samples^{23,24,25}, single crystal samples^{15,16,17,18,26} formerly reported have a little bit lower transition temperature at around $38\ \text{K}$. It is noted that our samples are not an exceptional case. This lower T_c in single crystals was thought to be caused by contamination from container materials (BN, Mo, Nb). From the quantitative analysis using an electron probe micro-analyzer (EPMA), however we found that there was no contamination in the samples from the container, which was Mo and SUS304 in our case. According to this analysis, the composition is rather ideal without particular stoichiometry shift, therefore, the quality check of the single crystals is an urgent need in more detail. Figure 3(b) shows the magnetic hysteresis curves $M(H)$ at $5\ \text{K}$ for applied fields up to $2\ \text{T}$ for $H//ab$ and for $H//c$, indicating the characteristic curve of type-II superconductors. There is an asymmetry between the ascending and the descending branches at $H \leq 0.1\ \text{T}$, which has been also observed in the magnetic hysteresis measurements on single crystals²¹.

Figure 4 shows the temperature dependence of magnetization $M(T)$ curves on warming after field cooling the sample for (a) $H//ab$ in magnetic field up to $5\ \text{T}$ and (b) $H//c$ in magnetic field up to $2.5\ \text{T}$. The superconducting transition shifts to lower temperatures as the field increased. The superconducting transition in fields is determined by extrapolating the $M(T)$ curve lineally and by finding the crossing point to the horizontal line

TABLE I: Comparison of physical parameters with single crystals prepared by different methods.

Parameter	Our sample	J. Karpinski <i>et al</i> ^{19,21,27}	S. Lee <i>et al</i> ^{15,28}	M. Xu <i>et al</i> ¹⁸	K. H. P. Kim <i>et al</i> ^{17,20}
$a(\text{\AA})$	3.0863(4)	3.085(1)	3.0851(5)	3.047(1)	3.09±0.06
$c(\text{\AA})$	3.5178(4)	3.518(2)	3.5201(5)	3.404(1)	
R	0.020	0.015-0.020	0.018		
R_w	0.027	0.015-0.020	0.025		
$T_c(\text{K})$	38	38-39	38.1-38.3	39	38
$H_{c2}^{ab}(0)(\text{T})$	13.6	14.5 ^a , 23 ^b	21-22	19.8	
$H_{c2}^c(0)(\text{T})$	3.4	3.18 ^a , 3.1 ^b	7.0-7.5	7.7	3.5
$\gamma(\text{T})$	1(T_c)-4.0(25 K)	1(T_c)-4.2(22 K) ^a , 2.8(35 K)-6(15 K) ^b	2.2(T_c)-3(30 K)	2.6(0 K)	2(T_c)-4.4(22 K)

^aValues determined from the magnetic measurement^bValues determined from the magnetic torque measurementFIG. 3: (a)Temperature dependent magnetization curves for the MgB₂ single crystal. FC and ZFC denote the field cooling and zero field cooling curves, respectively. (b)The magnetic hysteresis curves $M(H)$ at 5 K.

extended from the normal state. From this data, Fig. 5(a) shows the upper critical field of MgB₂ for applied fields $H//ab$ and $H//c$. H_{c2}^{ab} show a non-linear temperature dependence near T_c and then rise rapidly at lower temperatures. H_{c2}^c increases linearly with decreasing temperature. From Fig 5(a), $\gamma = H_{c2}^{ab}/H_{c2}^c$ is found to be temperature dependent, and it is shown in Fig 5(b).

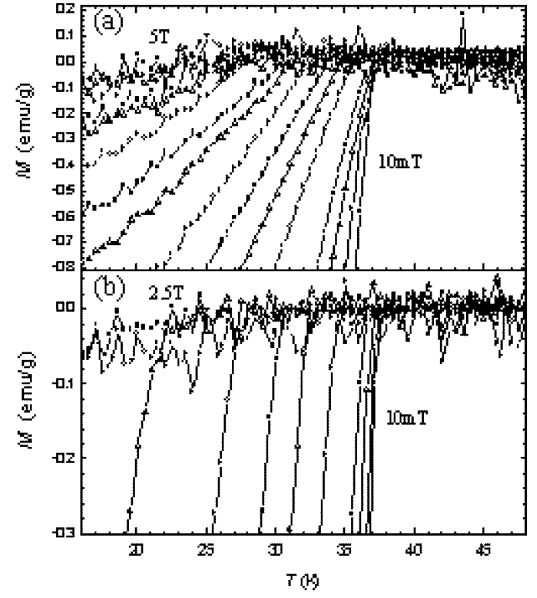


FIG. 4: (a) and (b) Temperature dependence of the magnetization on zero-field cooling in the several fields.

It increases from about 1 near T_c to 4.0 at 25 K. The extrapolation of H_{c2}^{ab} and H_{c2}^c lines to the zero temperature axis yields $H_{c2}^{ab}(0) \sim 13.6$ T, and $H_{c2}^c(0) \sim 3.4$ T with $\gamma \sim 4.0$. These values are similar to the previous results obtained from magnetic measurements on powder samples²⁹ or on single crystals^{19,20,21,22}, but don't agree with the reported γ -values determined from resistivity measurements on crystals^{10,11,15,16,17,18,30} and c -axis oriented films^{12,13,14}, which are around 1.1 to 3, as shown in Table I.

The specific heat was measured by a adiabatic heat pulse method in the magnetic field of 0 and 6 T in a temperature range between 2 and 60 K. The result of the specific heat as a function of temperature is shown in figure 6. The change in the specific heat in the T_c neighborhood is inserted as an inset in Fig 6. The critical temperature

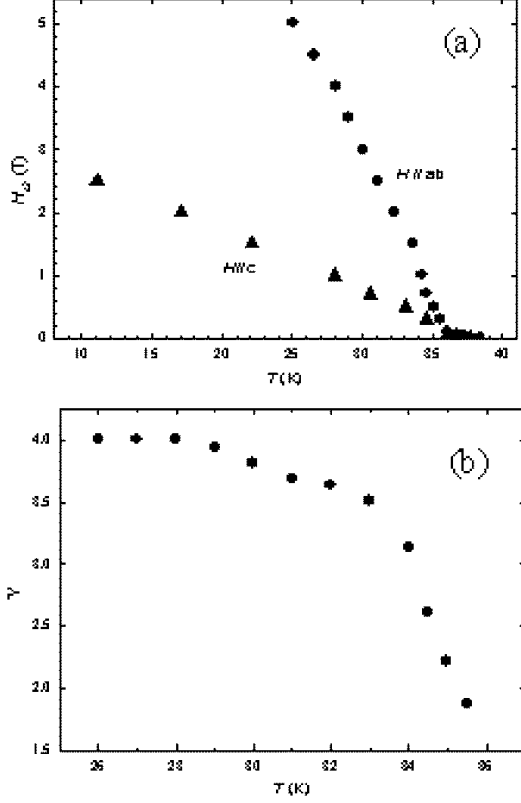


FIG. 5: (a) Upper critical field for H_{c2}^{ab} and H_{c2}^c determined from the onset of the superconductivity in Fig 4(a) and (b) as a function of the temperature. (b) Temperature dependence of upper critical field anisotropy $\gamma = H_{c2}^{ab}/H_{c2}^c$.

T_c defined by the mid point of the jump in the specific heat is 38.5 K, and the width of the jump is about 1 K. The value $\Delta C(T_c)/T_c$ of the jump of specific heat is $2.8 \text{ mJ/K}^2 \text{ mol}$. However, the jump of the specific heat was not observed in the magnetic field of 6 T in this scale. It is important to separate electronic specific heat from the entire specific heat to know the excitation of the electron system. It is assumed that the entire specific heat is composed of the specific heat of the electron system and the lattice system, $C(T) = C_e(T) + C_{ph}(T)$. The specific heat of the lattice system is expressed by $C_{ph}(T) = \beta T^3$ within the range of the temperature which is sufficiently lower than that of the Debye temperature θ_D . The electron specific heat is assumed to be $C_e(T) = \gamma T$ in the normal state. The plot of $C(T)/T$ vs. T^2 is shown in Fig. 7. However, it is clear that the expression of $C(T)/T = \gamma + \beta T^2$ in the normal state between 40 and 60 K in 0 T magnetic field and between 30 and 50 K in 6 T magnetic field. The higher-order term is then added in the expression to correct the specific heat of the lattice: it is approximated by $C_{ph}(T) = \beta T^3 + \beta_5 T^5$. The electronic specific heat was separated by extrapolat-

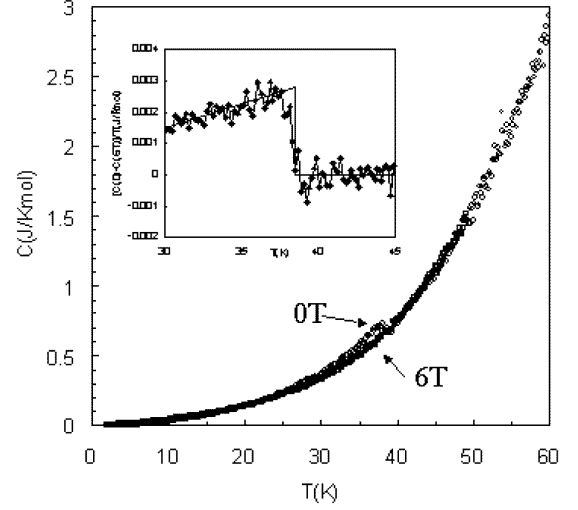


FIG. 6: Specific heat of MgB_2 under magnetic field of range 2-60 K of temperature, 0 and 6 T. Inset: Expansion of T_c neighborhood.

ing it to a lower temperature region by using the specific heat of the lattice by which the specific heat of the normal state was corrected. This fitting gave the result of $\gamma = 3.51 \text{ mJ/K}^2 \text{ mol}$, $\beta = 6.76 \times 10^{-6} \text{ J/K}^4 \text{ mol}$ and $\beta_5 = 1.08 \times 10^{-9} \text{ J/K}^6 \text{ mol}$, giving 0.8 to the jump $\Delta C(T_c)/\gamma T_c$ of the specific heat normalized by γT_c , and is different from 1.43 of BCS theory. The temperature dependence of the superconducting electronic specific heat $C_{es}(T)$ which had been obtained by subtracting the specific heat of the lattice from the entire specific heat of the superconducting state was shown in Fig. 8. The temperature dependence of the electronic specific heat of the superconducting state in zero magnetic field deviates strongly from the specific heat of the BCS theory as seen in Fig. 8. It is smaller than the value of the BCS theory in $20 \text{ K} \leq T \leq T_c$. But it is larger than the value of the BCS theory in $T \leq 20 \text{ K}$. A gradual jump of the specific heat, which extended in a wide range of temperature 20-28 K under the magnetic field of 6 Tesla was observed. The critical temperature in this magnetic field agrees roughly to the one obtained by the experimental result of the upper critical magnetic field measurement¹⁸.

The entropy in the superconducting state can be obtained by using $S(T) = \int C_e(T)/T dT$ under the condition that the entropy of superconducting state and normal state should be equal at T_c , i.e., $S_s(T_c) = S_n(T_c)$. The temperature dependencies of the entropy in both states are shown in Fig. 9. Furthermore, the critical magnetic field $H_c(T)$ was obtained from the entropy of superconducting state and normal state by using the expression $\int S_n(T) - S_s(T) dT = H_c(T)^2/8\pi$.

In order to make the difference from the BCS theory clear, the deviation function $D(t) = H_c(t)/H_c(0) - (1-t^2)$ as shown in Fig. 10 where $t = T/T_c$. The BCS the-

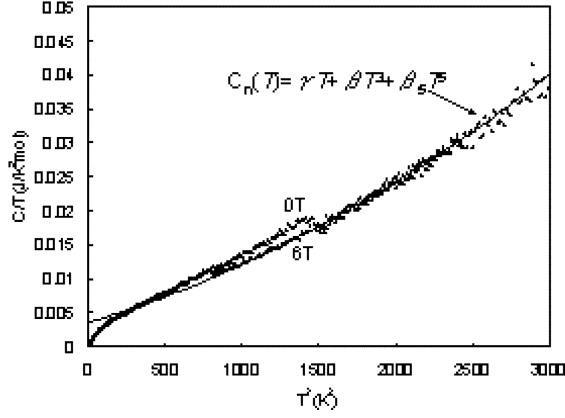


FIG. 7: $C(T)/T$ in magnetic field 0 and 6 T plotted as a function of T^2 . The solid line is a curve by which the fitting is done by $C_n(T) = \gamma T + \beta T^3 + \beta_5 T^5$ and the specific heat of normal state is extended to the low temperature.

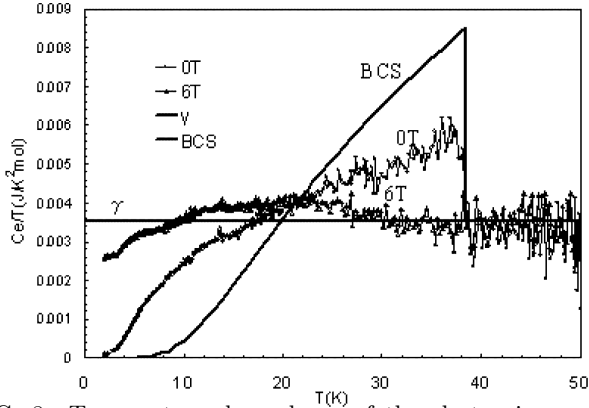


FIG. 8: Temperature dependence of the electronic specific heat C_{es} in magnetic field 0 and 6 T. The BCS theory was shown in the solid line and the specific heat of normal state was shown in the horizontal dotted line.

ory assumes the weak electron-phonon interaction, the isotropic Fermi surface and the isotropic interaction. The difference between the superconducting electronic specific heat and the one of the BCS theory shown in Figure 10 may be caused by the strong coupling effect, and/or the anisotropy of the Fermi surface and the anisotropy of the interaction. However, the effect of the electron-phonon coupling and anisotropy cause the opposite effect in the normalized jump of the specific heat $\Delta C(Tc)/\gamma Tc$ and the deviation function $D(t)$. That is, when the coupling becomes stronger, the value of $\Delta C(Tc)/\gamma Tc$ grows more than the BCS value of 1.43, and the deviation function $D(t)$ shifts from the BCS curve to a positive direction. On the other hand, when the anisotropy becomes, the value of $\Delta C(Tc)/\gamma Tc$ becomes smaller than the values of BCS, and $D(t)$ is changed in a negative direction^{31,32,33}. Value 0.8 of the jump of the normalized specific heat was smaller than the value of BCS and show the deviation function $D(t)$ in Fig. 10 which appeared

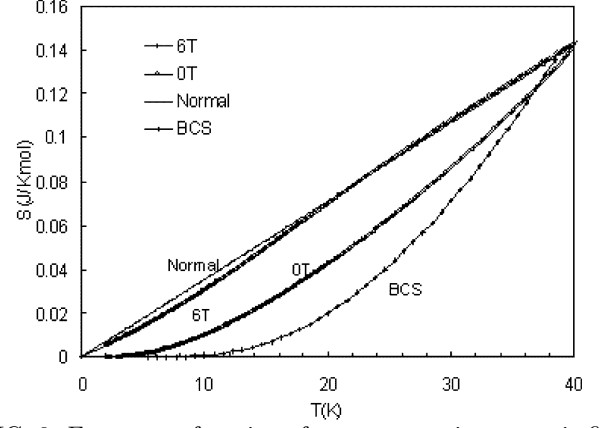


FIG. 9: Entropy as function of temperature in magnetic field of 0 and 6 T. The entropy of normal state and the BCS theory was shown.

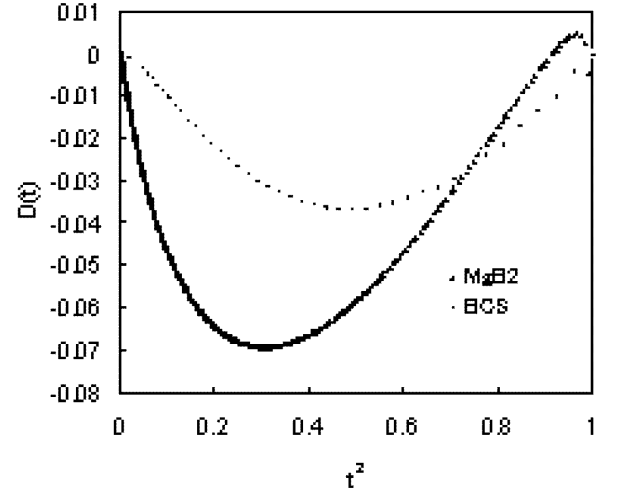


FIG. 10: Temperature dependence of the deviation function $D(t)$: $D(t) = H_c(t)/H_c(0) - (1-t^2)$, $t = T/Tc$.

in more negative direction than the BCS curve.

According to the results shown above the superconducting state of MgB_2 exhibits rather strong anisotropy of order 4 at low temperature. This result agrees with the result of the specific heat measurement in other groups⁶. The experimental result predicting the existence of two gaps has been reported in the result of tunneling microscopy⁸. Models of the two-zone or the multi-zone where the anisotropy is treated by dividing the Fermi surface, when the anisotropy of both the Fermi surface and the coupling becomes stronger, might be a good model. The anisotropy effect in the framework of the two-zone model was discussed³⁴. In that case, the value of the energy gap is different in each zone. Therefore, the specific heat would have the jump at a different temperature to which the energy gap of each zone opens. Though the temperature dependency of specific heat changes largely by the inter-zone scattering of conduction electrons, it

differs largely from specific heat of the single-zone (single-band) isotropic superconductor. Part of the large electronic specific heat C_{es} at the low temperature in Fig. 8 depends on the existence of a small energy gap it to be possible to excite even at the low temperature.

In summary, we reported on the results of measurement and the analysis of the specific heat of polycrystalline MgB_2 and the magnetic properties of single crystalline MgB_2 . The behavior of the superconducting electronic specific heat and the deviation function indicate

that the superconducting state of this MgB_2 is a strong anisotropy superconducting state, which is different from the BCS theory. From the magnetization measurement on single crystals, the upper critical field anisotropy ratio $\gamma = H_{c2}^{ab}/H_{c2}^c$ is found to be increased from about 1 near T_c to 4.0 at 25 K.

We would like to thank K. Yamawaki, K. Noda, K. Ishikawa, H. Saito, Y. Takano, and K. Ohshima for useful discussions.

-
- * Corresponding author: Tel.+81-45-924-5383; Fax.+81-45-924-5339
E-mail address: machida@lipro.rlem.titech.ac.jp
- 1 J. Nagamatsu, N. Nakagawa, T. Muranaka, Y. Zenitani, and J. Akimitsu, *Nature* **410**, 63 (2001).
 - 2 S. L. Bud'ko, G. Lapertot, C. Petrovic, C. E. Cunningham, N. Anderson, and P. C. Canfield, *Phys. Rev. Lett.* **86**, 1877 (2001).
 - 3 J. W. Quilty, A. Yamamoto, and S. Tajima, *Phys. Rev. Lett.* **88**, 087001 (2002).
 - 4 J. Kortus, I. I. Marzin, K. D. Belashchenko, V. P. Antropov, and L. L. Boyer, *Phys. Rev. Lett.* **86**, 4656 (2001).
 - 5 A. Y. Liu, I. I. Marzin, and J. Kortus, *Phys. Rev. Lett.* **87**, 087005 (2001).
 - 6 F. Bouquet, R. A. Fisher, N. E. Phillips, D. G. Hinks, and J. D. Jorgensen, *Phys. Rev. Lett.* **87**, 047001 (2001).
 - 7 P. Szabó, P. Samuely, J. Kačmarčík, T. Klein, J. Marcus, D. Fruchart, and S. Miraglia, *Phys. Rev. Lett.* **87**, 137005 (2001).
 - 8 F. Giubileo, D. Roditchev, W. Sacks, R. Lamy, D. X. Thanh, and J. Klein, *Phys. Rev. Lett.* **87**, 177008 (2001).
 - 9 M. Iavarone, G. Karapetrov, A. E. Koshelev, W. K. Kwok, G. W. Crabtree, and D. G. Hinks, *cond-mat/0203329*.
 - 10 F. Simon, A. Jánossy, T. Fehér, F. Murányi, S. Garaj, L. Forró, C. Petrovic, S. L. Bud'ko, G. Lapertot, V. G. Kogan, et al., *Phys. Rev. Lett.* **87**, 047002 (2001).
 - 11 O. F. de Lima, R. A. Ribeiro, M. A. Avila, C. A. Cardoso, and A. A. Coelho, *Phys. Rev. Lett.* **86**, 5974 (2001).
 - 12 S. Patnaik, L. D. Cooley, A. Gurevich, A. A. Polyanskii, J. Jiang, X. Y. Cai, A. A. Squitieri, M. T. Naus, M. K. Lee, J. H. Choi, et al., *Superconduct. Science Techn.* **14**, 315 (2001).
 - 13 M. H. Jung, M. Jaime, A. H. Lacerda, G. S. Boebinger, W. N. Kang, H. J. Kim, E. M. Choi, and S. I. Lee, *Chem. Phys. Lett.* **343**, 447 (2001).
 - 14 R. J. Olsson, W. K. Kwok, G. Karapetrov, M. Iavarone, H. Claus, C. Peterson, G. W. Crabtree, W. N. Kang, H. J. Kim, E. M. Choi, et al., *cond-mat/0201022*.
 - 15 S. Lee, H. Mori, T. Masui, Y. Eltsev, A. Yamamota, and S. Tajima, *J. Phys. Soc. Jpn.* **70**, 2255 (2001).
 - 16 A. K. Pradhan, Z. X. Shi, M. Tokunaga, T. Tamegai, Y. Takano, K. Togano, H. Kito, and H. Ihara, *Phys. Rev. B.* **64**, 212509 (2001).
 - 17 K. H. P. Kim, J. H. Choi, C. U. Jung, P. Chowdhury, H. S. Lee, M. S. Park, H. J. Kim, J. Y. Kim, Z. Du, E. M. Choi, et al., *Phys. Rev. B.* **65**, 100510 (2002).
 - 18 M. Xu, H. Kitazawa, Y. Takano, J. Ye, K. Nishida, H. Abe, A. Matsushita, N. Tsujii, and G. Kido, *Appl. Phys. Lett.* **79**, 2779 (2001).
 - 19 M. Angst, R. Puzniak, A. Wisniewski, J. Jun, S. M. Kazakov, J. Karpinski, J. Roos, and H. Keller, *Phys. Rev. Lett.* **88**, 167004 (2001).
 - 20 U. Welp, G. Karapetrov, W. K. Kwok, G. W. Crabtree, C. Marcenat, L. Paulius, T. Klein, J. Marcus, K. H. P. Kim, C. U. Jung, et al., *cond-mat/0203337*.
 - 21 M. Zehetmayer, M. Eisterer, H. W. Weber, J. Jun, S. M. Kazakov, J. Karpinski, and A. Wisniewski, *cond-mat/0204199*.
 - 22 A. V. Sologubenko, J. Jun, S. M. Kazakov, J. Karpinski, and H. R. Ott, *Phys. Rev. B.* **65**, 180505 (2002).
 - 23 C. U. Jung, M. S. Park, W. N. Kang, M. S. Kim, S. Y. Lee, and S. I. Lee, *Physica C* **353**, 162 (2001).
 - 24 Y. Takano, H. Takeya, H. Fujii, H. Kumakura, T. Hatano, and K. Togano, *Appl. Phys. Lett.* **78**, 2914 (2001).
 - 25 J. D. Jorgensen, D. G. Hinks, and S. Short, *Phys. Rev. B.* **63**, 224522 (2001).
 - 26 A. V. Sologubenko, J. Jun, S. M. Kazakov, J. Karpinski, and H. R. Ott, *cond-mat/0111273*.
 - 27 J. Karpinski, M. Angst, J. Jun, S. M. Kazakov, R. Puzniak, A. Wisniewski, J. Roos, H. Keller, A. Perucchi, L. Degiorgi, et al., *cond-mat/0207263*.
 - 28 Y. Eltsev, S. Lee, K. Nakao, N. Chikumoto, S. Tajima, N. Koshizuka, and M. Murakami, *cond-mat/0202133*.
 - 29 S. L. Bud'ko and P. C. Canfield, *cond-mat/0201085*.
 - 30 G. K. Perkins, J. Moore, Y. Bugoslavsky, L. F. Cohen, J. Jun, S. M. Kazakov, J. Karpinski, and A. D. Caplin, *cond-mat/0205036*.
 - 31 J. R. Clem, *Ann. Rev.* **40**, 286 (1966).
 - 32 H. Padamsee, J. E. Neighbor, and C. A. Shiffman, *J. Low Temp. Phys.* **12**, 387 (1973).
 - 33 D. G. Gubser, *Phys. Rev. B.* **6**, 827 (1972).
 - 34 P. Entel, *Z. Physik. B.* **24**, 263 (1976).